Available online at www.sciencedirect.com
ScienceDirect
Journal of Applied Geophysics 62 (2007) 47–57
JOURNAL OF APPLIED GEOPHYSICS
www.elsevier.com/locate/jappgeo

Identification of the gravitational boundary in weathered gneiss by geophysical survey: La Clapière landslide (France)

H. Jomard, T. Lebourg, E. Tric *

Laboratoire Géosciences Azur, CNRS/UNSA, Université de Nice - Sophia Antipolis 250 rue A. Einstein, 06560 Valbonne, France

Received 26 September 2005; accepted 28 July 2006

Abstract

Geophysical surveys were conducted on the unstable upper part of the La Clapière landslide in the French Alps (Alpes Maritimes). Electrical resistivity and seismic measurements were carried out over a 2-year period to obtain, for the first time on this landslide, general information on the weathered zones, slipping surface and the network of water drainage. This geological information is derived from two different surveyed areas presented in this paper. For the characterisation and quantification of the weathering, the data showed a very good correlation between the electrical resistivity and the velocity of the direct waves which is dependant on the quality of the rock, and put into context by the survey of geological and structural outcrops. This comparison made it possible to differentiate the weathered zones from unweathered zones. The electrical resistivity profiles also allowed mapping of the weathering zones at depth, and provided information on channeling of the water within the slope and on the depth of the slip surface. Thus, the origin of the instability of the upper part of the La Clapière landslide seems to be strongly associated to the water circulation. The maximum depth of the slipping surface in the uppermost part of the landslide is around 30 m. Moreover, for the first time we have also identified from electrical resistivity tomography, (1) a boundary, at a depth of about 90±10 m, which could be the depth of the slipping surface of the La Clapière landslide and (2) a possible perched aquifer.
© 2006 Elsevier B.V. All rights reserved.

Keywords: Geophysical investigation; Landslide; Resistivity imaging; Slipping surface; Weathered materials; Electrical tomography

1. Introduction

The understanding of rupture processes in deep seated landslides and hence the prediction of the evolution of such phenomena is difficult for two main reasons. The first one arises from the difficulty in estimating the mechanical behaviour of the affected rock mass which is very different from that of rock samples we can study in the laboratory. This is mainly true in the upper part of the slope subjected to weathering (Lebourg et al., 2003). The second reason is due to the necessity of taking into account the 3D geometry of the phenomenon, and particularly the geological discontinuities affecting the rock mass. The geometry and the structure can be obtained from geomorphological, geotechnical, geophysical, and mechanical data. In order to achieve this task, both direct and indirect investigations must be performed. The first approach is geomorphological, because it allows on the one hand to conceptualize a model of the studied site and, on the other hand to define a protocol of study of the site (Hutchinson, 1988; Chigira et al., 2003; D'amato Avanzi et al., 2004; Catani et al., 2005; Dymond et al., 2006; Komac, 2006). Concerning

* Corresponding author.
E-mail address: tric@geoazur.unice.fr (E. Tric).

0926-9851/$ - see front matter © 2006 Elsevier B.V. All rights reserved.
doi:10.1016/j.jappgeo.2006.07.003

direct investigations, geotechnical methods may be used to obtain accurate data allowing slip surfaces to be located, but the high cost of such methods implies that they are not always suitable. Thus, an overall structural interpretation of the landslide is not easy and sometimes impossible. For this reason geophysical methods such as electrical resistivity tomography are employed (Mauritsch et al., 2000; Roth et al., 2002). Its main advantage is that it is possible to measure the ground response along continuous (or pseudo-continuous) profiles located on the ground surface in order to obtain 2D and 3D imagery of the structure with an identification of weathered zones that can be associated with lithologic, hydrologic and mechanical characteristics. Nevertheless, the technique requires calibration and validation and complementary information (geomorphologic, hydrogeologic, tectonic, etc.) or the application of other geophysical methods (seismic reflection and refraction, gravity) to validate the results obtained. Some recent works have shown that the application of resistivity methods can reveal very important details of the weathered zones, the hydrological system, and geological structure (Robain et al., 1996; Lebourg et al., 1999; Ritz et al., 1999; Jongmans et al., 2000; Sumanovac and Weisser, 2001; Lebourg and Frappa, 2001; Godio and Bottino, 2001; Wise et al., 2003; Perrone et al., 2004; Lebourg et al., 2005; Rey et al., 2006; Godio et al., 2006; Sumanovac, 2006). However, this method has been rarely used on deep seated landslides because of logistical difficulties with using resistivity equipment in steep and unstable terrain.

The purpose of this work was to investigate whether the electrical resistivity tomography could provide accurate information on the weathered zones, slipping surface, major discontinuities and the drainage network in the upper part of the La Clapière landslide (Alpes Maritimes, France). Although numerous studies have been carried out on this landslide (hydrological, geologic, tectonic, topographic) (Follacci, 1987; Ivaldi et al., 1991; Compagnon et al., 1997; Guglielmi et al., 2000; Cappa et al., 2004)), only one geophysical survey has been performed at the foot of this landslide (Lebourg et al., 2005). For this reason, we decided to undertake, for the first time, such a study by applying the geophysical approach to the La Clapière landslide and more precisely to the more unstable part located at the top.

2. Geographical, geomorphological, geological and hydrogeological setting

The La Clapière landslide is located in the French Southern Alps (Fig. 1), downstream from the village of Saint-Etienne-de-Tinée, at the edge of the Mercantour massif. This landslide affects an area around 100 ha between 1100 and 1800 m of elevation and mobilizes a volume of rock about of 60 million m^3. It is bordered on its northwestern side by the Tenibres river and to its southeastern side by the Rabuons river, flowing into the Tinée river. The three valleys define a N010°E trending prismatic geometry that allows a 3-dimensional view of the unstable area. The prism culminates at an elevation of 2200 m. Elevations of surrounding crests and peaks reach 3000 m.

The landslide currently overlaps the quaternary alluvial deposit of the Tinée River and affects the hercynian basement rocks composed mainly of migmatitic gneiss (Follacci, 1987, 1999). A subhorizontal bar of metadiorite, called the Iglière bar, crosses the landslide at an average elevation of 1350 m (Fig. 2). All geological units have a hercynian foliation with a near subhorizontal dip at the edges of the landslide and a 10° to 30° dip to the NE within the landslide (Follacci, 1987, 1999; Gunzburger and Laumonier, 2002; Delteil et al., 2003). The metamorphic foliation in the La Clapière zone appears undulated and microfolded. At the top of the slope, between elevations of 1700 and 2200 m, metamorphic rocks are weathered over a thickness ranging from 50 to 200 m. In the middle and at the foot of the slope, the gneisses are fractured. This landslide is largely fractured with three characteristic directions of faults (Guglielmi et al., 2000) which are N10–30°E, N90°E and N110–140°E with a dip angle close to 90°. A fault with a N20 direction divides the landslide into two parts.

The landslide is bounded at the top by a main scarp of 60–80 m height which forms two lobes, an upper NE lobe and an upper NW lobe (Follacci, 1987). Two secondary scarps have developed within the landslide. One of the scarps has a N120 direction and is located at an average elevation of 1500 m, the other scarp having developed since 1987 along a N90 fault just under the top NW lobe (Fig. 1).

In the upper NE lobe, a secondary landslide is superimposed on the major one. This area corresponds to a 5 million m^3 volume which has completely lost its cohesion and which behaves like a block landslide sliding along its own failure surface which is shallower than that of the main landslide. It overlaps the main landslide. The downward movement of this compartment ranges between 100 and 380 mm $year^{-1}$. This area is the site of the geophysical prospecting presented in this paper. The upper part of the landslide between the headscarp and the Iglière bar has a characteristic morphology in decametric steps (Follacci, 1987). This landslide has probably been active since the beginning of the 20th century. The first studies of the La Clapière landslide were carried out in 1977. Distance

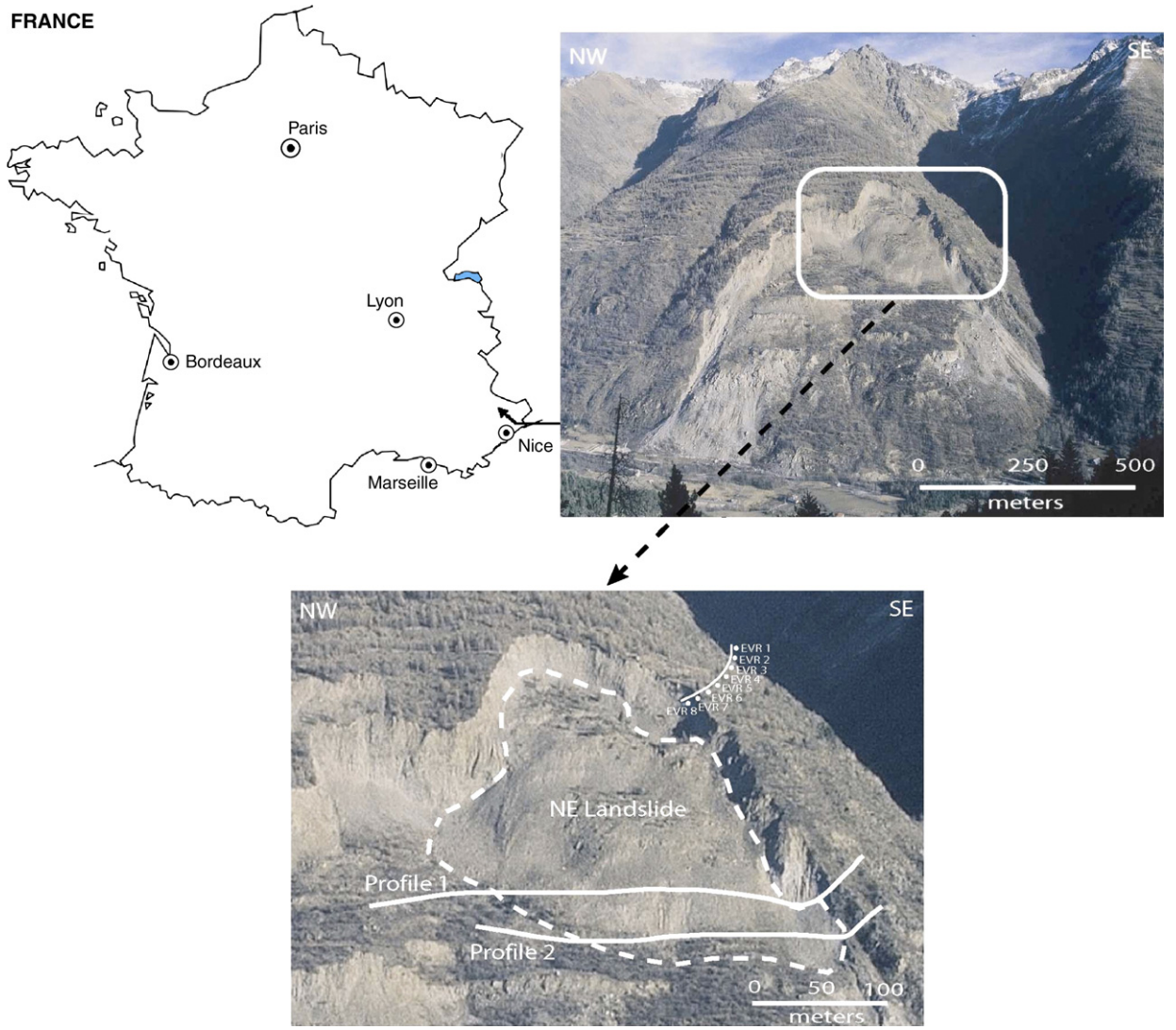

Fig. 1. The "La Clapière" landslide in 1998, localisation of the studied area (photo from G. Sève, CETE de Nice). A zoom of this area is done in order to locate the different geophysical surveys on the North–East section of La Clapiere landslide, which is actually the more unstable part of the slope.

measurements have been regularly acquired since 1982. These data indicate velocities of 1 cm/day on average. Two accelerations have been registered: one in autumn 1987 with velocities greater than 10 cm/day and one at the beginning of 1997 with velocities greater than 5 cm/day (Follacci, 1999). Moreover, these measurements reveal a seasonal response of the landslide characterised by an acceleration of movements correlated to snow melting (Follacci, 1987, 1999). For a few years, this distance monitoring has been combined with other types of investigations: hydrogeological studies (Compagnon et al., 1997; Guglielmi et al., 2000), remote sensing (Casson et al., 2003; Squarzoni et al., 2003) and subsurface geophysical investigations (Lebourg et al., 2003). Different types of geometric, mechanic or hydromechanic models have been derived from these data sets (Merrien-Soukatchoff et al., 2001; Cappa et al., 2004) but none of them visualise the morphology of the main slip surface geometry. Based on cross-sectional geometry, the depth of the failure surface may not exceed 100–200 m (do not link Fig. 2 in Cappa et al., 2004), but no data exist to confirm this estimation, In this study we present the morphology and the image of the slip surface of the superimposed landslide affecting the upper part of the NE lobe.

The La Clapière slope itself is affected by many tectonic discontinuities, a complete description of which is reported in Gunzburger and Laumonier (2002). The major fractures are subvertical N20 faults intersecting the whole slope far

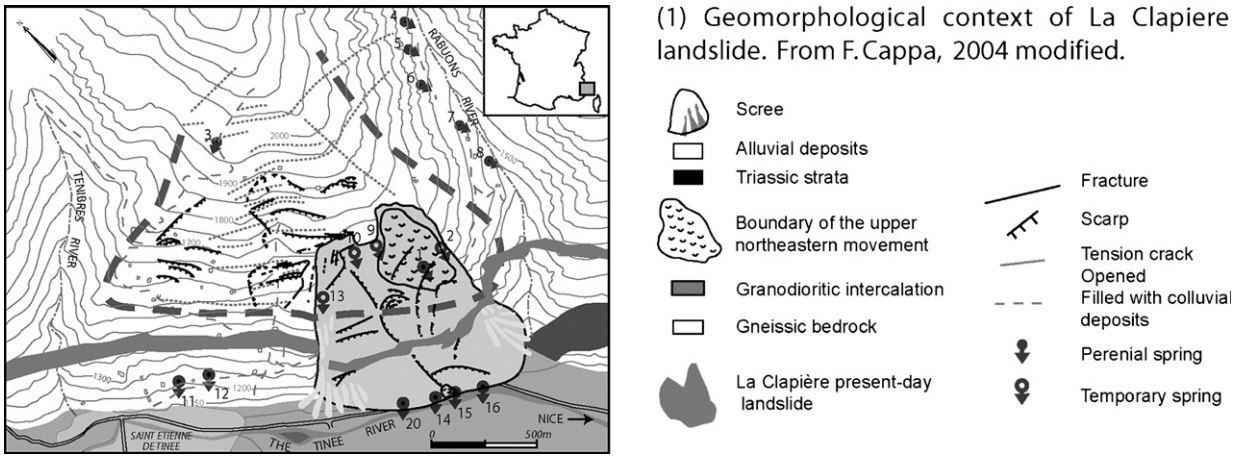

Fig. 2. Geological and geomorphological maps of Clapiere landslide from Cappa et al. (2004).

away from the active landslide and delimiting several parallel N20 slices, several hundred meters wide. The displacements measured by the monitoring system also have on average a N20 orientation. This suggests that faults play the role in guiding the deformation and also that they aid water drainage.

From the hydrogeological point of view, the landslide can be regarded as a discontinuous fractured reservoir. Water flows into fractures whose openings depend on the depth and on the structure of the slope. The landslide can be taken as a highly permeable fractured reservoir because the displacements induce the formation of large volumes of pore space inside opened fractures, breccias and blocks. The area is characterised by several springs (perennial and temporary). Some of these springs emanate directly from the basement along faults of different directions or in the weathered topsoil. Thus, the landslide is drained at its foot by a group of perennial springs with a total discharge of between 0.25 and 0.35 l s^{-1} (springs 14, 25, 16, 20 in Fig. 2). In the landslide, another perennial spring rises at the foot of the northeastern compartment at an elevation of 1550 m, and has a discharge of between 0.1 and 0.3 l s^{-1} (spring 1 in Fig. 2). This spring is located in our study area. After periods of long precipitation, some temporary spring rise occurs at the same elevation (springs 2, 9, 10, 13 in Fig. 2). All these temporary springs rise along faults or at the bottom of major tension cracks filled with colluvial deposits. All the streams that originate from the perched springs (springs located in the upper part of the landslide) are interrupted a few hundred meters downstream (Cappa et al., 2004). This mean that all the waters reinfiltrate the main landslide. Water chemistry studies carried out by Guglielmi et al. (2000, 2005) and Cappa et al. (2004) suggest the presence of two main flowpaths in this landslide: (1) flow through low permeability Triassic deposits pinched under the foot of the landslide, (2) flow through a more permeable fissured basement. These differences in the landslide drainage can be correlated with the different mechanical behaviour: high sliding speeds at the top and medium and slow speeds at the base of the landslide (Follacci, 1999). From these data, Cappa et al. (2004) proposed a conceptual hydromechanical model of the slope, in which a doubly permeable aquifer is present with a small number of highly conductive fractures and a large number of poorly conductive fractures. The main hydromechanical effect originates from snowmelting in the upper part of the slope between 1800 and 2500 m. From this upper rechargeable area, the transit time through the perched saturated zone can reach 5–8 days, and an infiltration yield ranging from 0.4 to 0.8 l s^{-1} causes a generalized landslide acceleration. The transit time of the groundwater to the basal saturated zone is between 8 and 12 days. Thus, landslide velocities are characterised by very slow periods (velocities ranging from 1 to 5 mm day^{-1}) and acceleration periods. Acceleration amplitudes are higher in the upper part than in the basal one. For example, Cappa et al. (2004) measured velocity values of 44.3 mm day^{-1} in the upper part versus 14.9 mm day^{-1} in the basal part of the landslide during the 99/11/25 event. For a more complete description the reader is referred to the papers by Guglielmi et al. (1998, 2000, 2005) and Cappa et al. (2004).

3. Characterisation and quantification of weathering across the landslide boundary

3.1. Geophysical and mechanical methods

The eastern flank of the slope displays the entire evolution from weathered (nearest to the landslide) to

unweathered gneiss (sites Electric Valley Rabuons, EVR, in Fig. 1). In order to try to quantify this evolution, we carried out different approaches using a range of geophysical surveys and mechanical (triaxial) tests.

Geophysical methods used in this study were electric imagery and P-wave seismic. They were used in order to evaluate and quantify the apparent values of electrical resistivity and P-wave velocity associated with the quality of the rock and to differentiate the weathered rock from the unweathered rock by mechanical characteristics.

The electrical approach was carried out using an electrical quadrupole (4 electrodes) using the Wenner array with the Syscal instrument from IRIS Instruments. Once all the electrodes were aligned and spaced 0.5 m or 1 m, measurements were carried out, each one giving a value of apparent resistivity at a geographical point of reference. The quadrupole is moved along the profile to obtain apparent resistivity values at different locations.

To quantify the variation of P-wave velocities, a seismic tool (McSeis-3, Iris Instruments) was used, suitable for the small outcrop scale survey. The seismic source employed was a hammer. First arrival times were determined for each site where resistivity measurements were carried out. An apparent P-wave velocity value of the direct wave has been deduced from each measurement.

We carried out for all sites a mechanical characterisation tested by a geophysical survey. The mechanical parameters usually used in rock mechanics are not applicable here because of the breakdown of the material due to mass movement. We decided to study the gneissic material by a triaxial test approach, and the samples taken at outcrops were mainly composed of granular elements. The elements sampled in the gravitational faults are supporting the maximum shearing stress in the field. They are mainly composed granular gneissic material. Consolidated Drained (CD) tests have been performed to simulate the stress paths followed by granular material elements in the studied areas of the slope, from the weathered zone to the unweathered zones and that under drained conditions. The study was carried out to investigate the shear strength characteristics of material associated to the quantification of the weathered evolution with the production of fines and granular elements. These tests were performed using a Wykeham Farrance triaxial press of 50 kN with 3500 kPa cells. For each sample we realised about 4 tests at 100 kPa, 200 kPa, 300 kPa and 400 kPa, for a 25% maximum deformation and for 3 mm/mn velocity. The mechanical parameters calculated here are the effective internal friction angle (ϕ' in degree) and the effective cohesion (C', in kPa).

These parameters are classically used in the equation of the Mohr–Coulomb failure criterion: $\tau_{max} = C' + \sigma_N \cdot \tan\phi'$, where τ_{max} is the maximum shearing stress and σ_N the normal stress (Costet and Sanglerat, 1981). Rewritten using the applied stress (σ_V and σ_H) to the specimen during the triaxial shear test, it becomes:

$$\frac{\sigma_V - \sigma_H}{2} = \left(\frac{\sigma_V + \sigma_H}{2} + \frac{C'}{tg\phi'}\right) \cdot \sin\phi'$$

The failure of the specimen occurs at (σ_V, σ_H) values determined in the laboratory; parameters C' and ϕ' can be calculated by simple mathematical expressions.

3.2. Results and interpretation

The mechanical results are shown in Table 1 for four sites (EVR2, EVR4, EVR6, EVR8). We observe a decreasing effective cohesion from the unweathered area (effective cohesion of 36 kPa, site EVR2) to the weathered area (effective cohesion of 2 kPa, site EVR8) whereas in the same time the value of the internal angle of friction (ϕ') increases from 24.7° up to 28.4°, which confirms the great variability of the mechanical behaviour.

The physical significance of this evolution of the internal angle of friction is difficult to explain at present. However, Lebourg et al. (2004) studied the mechanical behaviour of the moraines from Aspe valley (Atlantic Pyrenees) and made similar findings by establishing relations between the effective internal angle of friction, the elongation factor and the roughness factor. The similarity between our results and their implies that the more we approach the weathered area of La Clapière landslide, the more the elongation of the grains becomes important. From a geological point of view, it is well known that hydrolysis of gneiss, which is mainly made up of quartz (tectosilicate) and mica (phyllosilicate), leads progressively to the destruction of mica. This alteration forms clays drained by infiltrating water. This

Table 1
Physical and mechanical parameters determined from La Clapière material by triaxial tests

Sample location	EVR8	EVR6	EVR4	EVR2
E	74±7 MPa	49±5 MPa	52±5 MPa	43±4 MPa
c'	2±2 kPa	11±2 kPa	26±3 kPa	36±3 kPa
ϕ'	28.4°±1.2	29.3°±1.2	25.7°±1.2	24.7°±1.3

The sample locations are indicated in Fig. 1. E_m: mean Young modulus, c': internal effective cohesion, ϕ': internal angle friction.

drainage can lead to an increase of the percentage of quartz in the rock matrix and consequently an increase of the elongation factor. Given that the effective internal angle of friction is related to the elongation factor (Lebourg et al., 2004), our results are in agreement with the fact that the increase of effective internal angle is correlated with the increase of the weathering which is generally characterised by low electrical resistivity and P-wave velocity.

Measurements of electrical resistivity and velocity of the direct waves were carried out on various zones of the slip and more precisely from the limit of the landslide to the unweathered zone (Fig. 1). The knowledge of resistivity values corresponding to different degrees of weathering is very important for the study of resistivity tomography on the landslide, and the interpretation of resistivity contrasts. Fig. 3 shows the variation of the apparent resistivity and the velocity of the direct wave according to the sites of study. These sites, regularly spaced (about 100 m), extend from the unweathered zone (Rabuons gully, site EVR1, Fig. 1) to the weathered zone (site EVR8 is on the slip). The change from unweathered zone to weathered zone is clearly observed between sites EVR3 and EVR4. We can observe a very good correlation of the two signals with the unweathered or weathered character of the rock. From these measurements, we can infer that the unweathered rock has a value of apparent resistivity of about 5000–6000 Ω m and a propagation velocity of about 2000 m/s, whereas the weathered rock has values of apparent resistivity decreasing to 1500–2500 Ω m and its propagation velocity to 600 m/s. These results are in agreement with mechanical data given in Table 1, which show that the more we approach the weathering area the more effective cohesion decreases and effective internal friction angle increases.

Thus it seems possible, for the La Clapière landslide, to distinguish from resistivity values a weathered material from an unweathered material, with a critical value of resistivity around 2000±500 Ω m. This weathering results from chemical weathering and/or mechanical weathering. Yet the relative proportion of these two mechanisms and the possibility to associate this weathering signal with electrical signal remain uncertain because the electrical response of a weathered formation is a function of many parameters such as the porosity, amount of fracturing, water content and degree of saturation. However, if we consider only the chemical weathering (hydrolysis of the silicate) and micromechanical weathering, an increased content of clay and corresponding decrease of the permeability should cause a decrease in the resistivity. This is in fact what we observe using the subsurface imaging techniques discussed earlier in this section. We can also consider only the mechanical weathering from an increase in the volume of the voids created by the breakdown of the rock generated during gravity-related deformation which should cause an increase in the measured resistivity. The main problem is to quantify the relative contributions of these two weathering processes. In this study, the decreasing of the resistivity seems mainly to be associated to the production of clay minerals versus the breakdown of the gneiss. Moreover, it is important to consider that the La Clapière site is a petrologically homogeneous zone. Thus, a very strong decreasing of resistivity in this zone could be also associated to the presence of water. The question of from which value of resistivity can the presence of

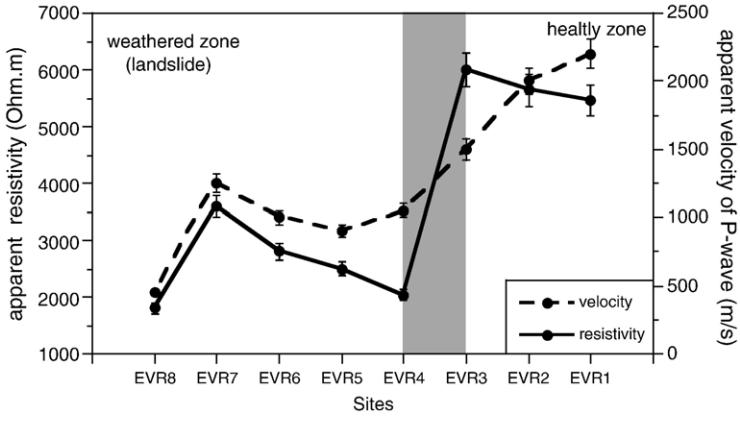

Fig. 3. Evolution of the electrical resistivity and the propagation velocity from the weathered zone of the landslide to the non-weathered zone. The grey band corresponds to the limit between weathered and unweathered zone.

water in the rock by implied is addressed in the following section.

4. Electrical resistivity tomography on the top of the La Clapière landslide

4.1. Electrical and tomography methods

The results of the previous study showed us a reduction in the resistivity when we pass from the unweathered zone to the weathered zone. The electric method using the panel resistivity method makes it possible to carry out a 2D tomography.

To obtain an image of the sub-surface it is necessary to carry out various measurements over a short period of time. This approach was undertaken with a multielectrode 2D device, using 48 electrodes separated by 10 m. We systematically used a pole–pole and dipole–dipole array, with measurement frequency of 4 Hz, for about 800 to 1100 measurements for each profile (no. 1 and no. 2, see Fig. 1). The 2D resistivity data were recorded using the Syscal R1 Plus imaging system (IRIS Instrument). The data are classically presented in the form of pseudo-sections (Edwards, 1977), which give an approximate picture of the subsurface resistivity. The data, once recorded, are transferred to and processed on a computer. Inversion of the data is required to obtain a vertical true resistivity section through the underlying structure (Loke and Barker, 1996; Bear et al., 1996). The field

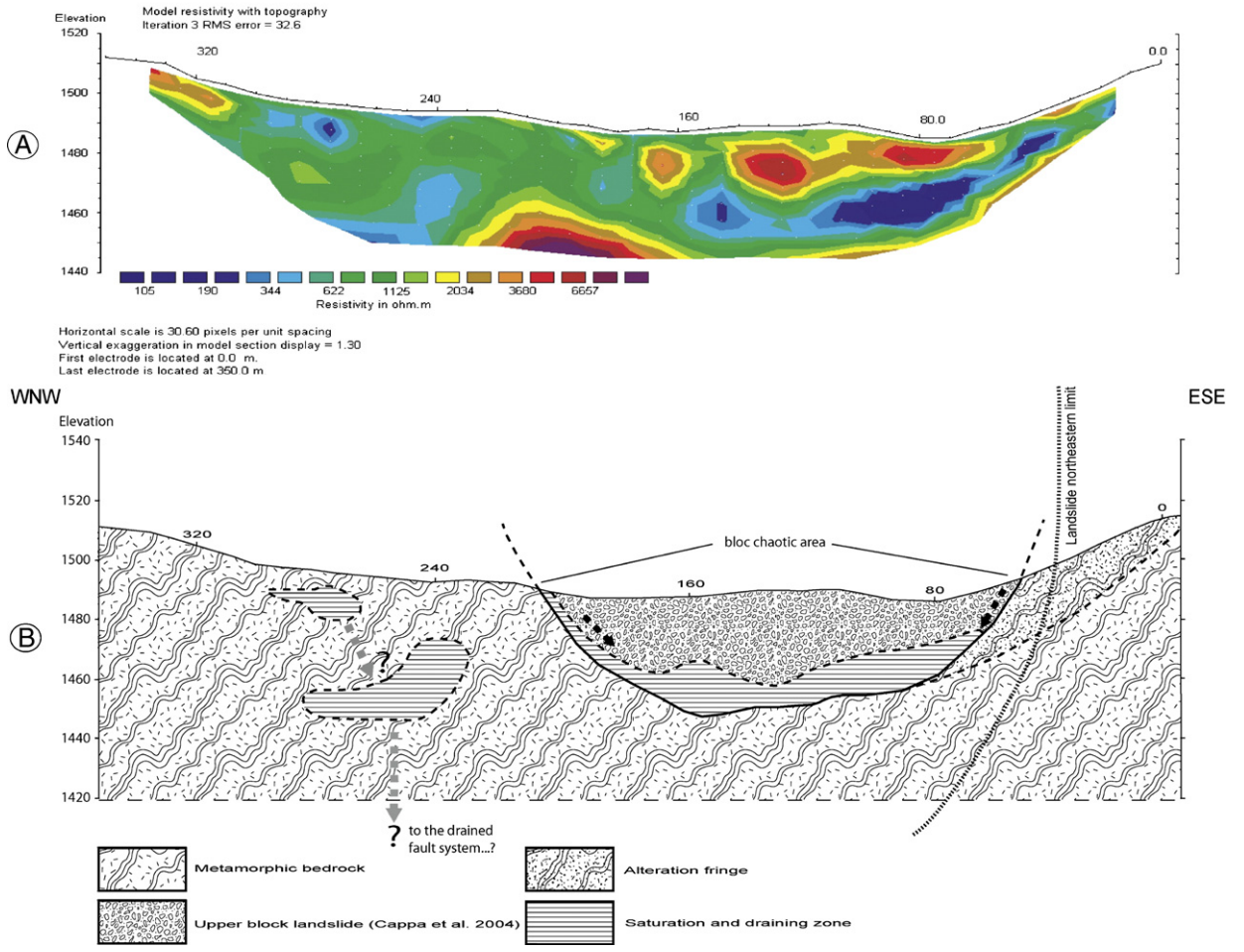

Fig. 4. (A) Electrical resistivity tomography obtained by the dipole–dipole survey on the NE landslide (profile no. 1). Very conductive zones are observed and can be interpreted as zone of drainage. We observe a good correlation between these zones and the presence in surface of two springs noted 1 and 2 in the text (see part 2). The result obtained after 6 iterations, as in Fig. 5, is equivalent to that obtained after 3 iterations. (B) Interpretation and localisation of the weathered zones of this profile. Hachured zones which correspond to very conductive zones observed in (A) could be considered as saturated zone and associated with slipping surface of the summit landslide.

data depicted as contoured pseudoresistivity sections were inverted with the $RES_{2D}INV$ software written by Loke (1997). Furthermore, the constraints provided by the topographic variations have been introduced into the inversion processing. To reduce the error on the resistivity interpretation, we systematically correlated each electrode to geological field observations. The interpretation of the resistivity cross section must be improved by a high resolution geological and structural study. This last aspect reduces the error of the interpretation.

Two profiles, separated by a distance of approximately 30 m, were obtained on the lower zone of the unstable and higher part of the landslide (Fig. 1). The profiles no. 1 and no. 2 were obtained in December 2003 and July 2004 respectively.

5. Geophysical results and interpretation

5.1. Profile no. 1 — dipole–dipole

This survey carried out in the higher part of the landslide made it possible to obtain information on the variations of resistivity to a depth of 50 m (Fig. 4). It was obtained during the winter of 2003. The interpretation identified three distinct geological objects:

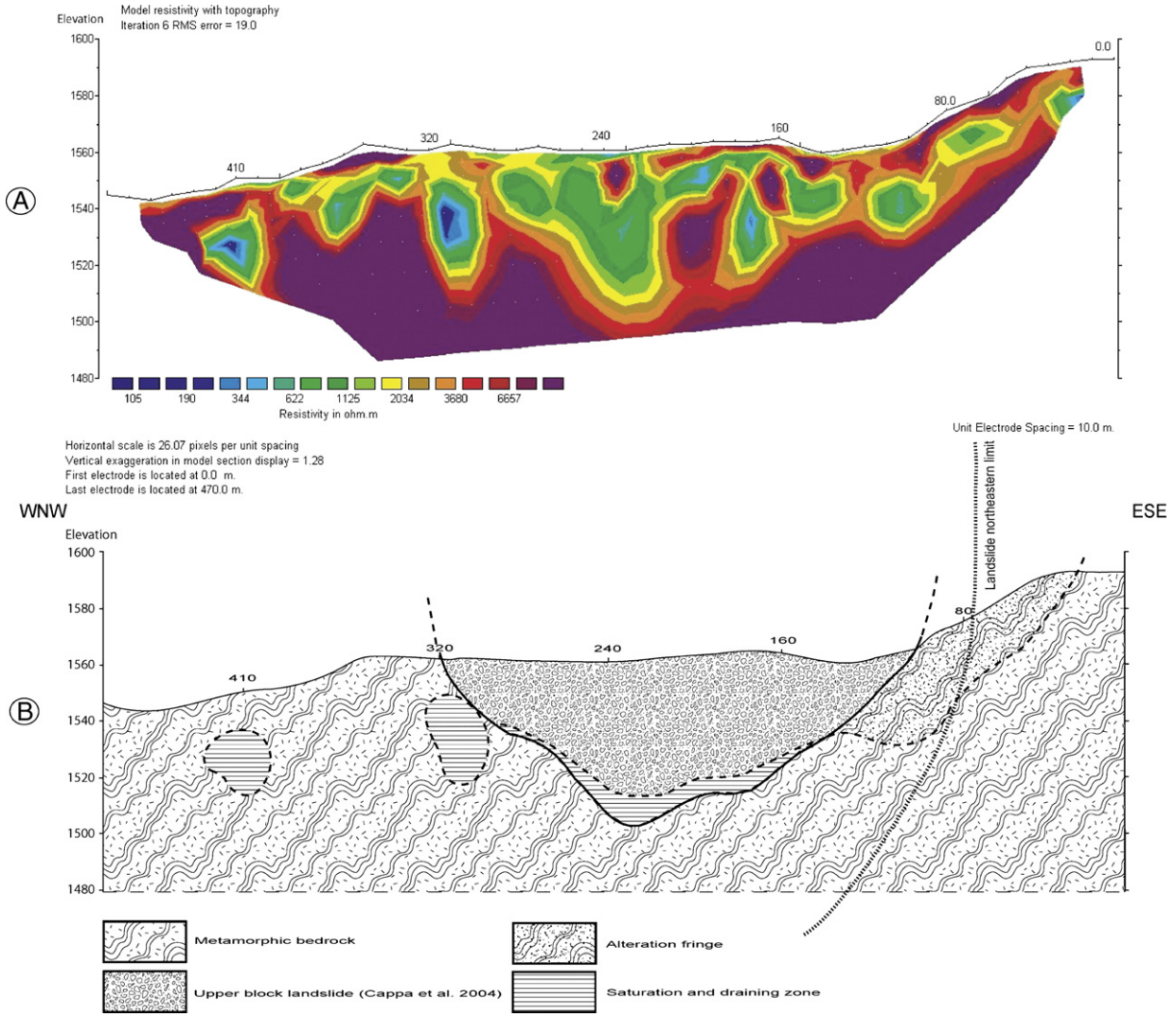

Fig. 5. (A) Electrical resistivity tomography obtained along a profile no. 2 by the dipole–dipole survey. This profile has been obtained in July 2004, 30 m above the profile no. 1 (Fig. 4). The image is comparable with the tomography obtained along the profile no. 1. (B) Hyrdogeological interpretation and localisation of the weathered zones of this profile.

1) Two zones of a few meters thickness characterised by very low resistivities (200–300 Ω m) and located below the horizontal points 240 m and 275 m (Fig. 4A). These two zones are interpreted as zones of drainage. The presence of faults acting as drainage is in agreement with recent hydrogeologic work (Guglielmi et al., 2002; Cappa et al., 2004) which has shown the relation between a perched aquifer, between elevation 1600 and 1800 m, and the deeper water table between 1100 and 1200 m (Cappa et al., 2004). Moreover, this interpretation is supported by the presence of springs which are located at the horizontal point 240 m and 20 m downslope of the electrode lines (see part 2, springs 1 and 2). Such results suggest the presence of a complex water channelisation within this part of the slope (Fig. 4B).
2) A very conductive zone located between the points 40 m and 200 m, of bowl-shaped form and maximum thickness of 30/40 m. This zone is characterised by electrical resistivities ranging from 100 to 300 Ω m which can be interpreted according to the field information as the slipping surface of the summit landslide (Fig. 4A, B).
3) After referring to the preliminary results (in Section 3.2), we can identify zones within the landslide where the gneisses are more or less weathered. For the weathered gneiss, the resistivity is around 1000 to 2000 Ω m, and for the unweathered gneiss, about 4000–5000 Ω m. It is quite obvious that this deterioration is in relation to the mass movement and to the occurrence of fractures in the gneiss rock mass. Thus, one observes within the slipped masses the zones known to be weathered (or decompressed) and the zones still relatively unweathered.

5.2. Profile no. 2 — dipole–dipole

This profile was obtained during July 2004, approximately 30 m above the profile no. 1 which was obtained in the winter of 2003. The resulting tomographic image is presented in Fig. 5A. It is comparable with the tomography obtained along the profile no. 1, but it presents differences owing to the fact that the profile was obtained during the summer and thus in a dry period. Thus, we observe a very large resistivity variability from 150 Ω m to 8000 Ω m with a vertical distribution in two zones. The first one, between 0 and about 20–30 m depth shows resistivity values generally lower than 1000 Ω m. The second, deeper, zone is characterised by very high resistivities (>7000 Ω m). This strong contrast could correspond to the boundary between weathered and unweathered gneiss and can be interpreted as the slipping surface of the summit landslide (Fig. 5B). This boundary is associated with the very low electrical resistivities observed in Fig. 4A obtained along the profile no. 1.

5.3. Profile no. 2 — pole–pole

This survey gives information on the variations of resistivity to a depth of 170 m (Fig. 6). We observe a

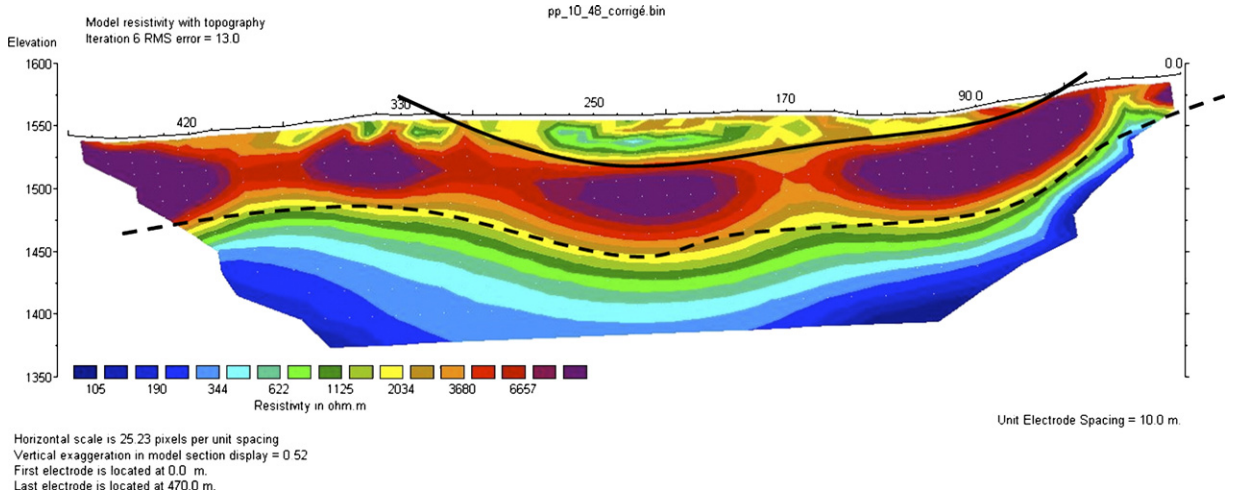

Fig. 6. Electrical resistivity tomography obtained along profile no. 2 by the pole–pole survey. This image shows three electrical structures: (1) the unstable part between 0 and 20–30 m of depth characterised in Fig. 4, (2) a layer of about 90 m thick which could corresponds to the principal structure of La Clapière and (3) a perched aquifer as suggested by Guglielmi et al. (2002) and Cappa et al. (2004).

very large resistivity variability from 100 Ω m to 7800 Ω m. with a vertical distribution in three zones. The first one, between 0 and 20–30 m corresponds to the unstable part characterised previously with the dipole–dipole surveys. The second one is about 90 m thick and characterised by high resistivities (≥5000 Ω m). This layer probably corresponds to the principal structure of the La Clapière landslide. Below this layer we found very low resistivities (≤150 Ω m) which may be associated with the presence of saturated material and may relate to the perched aquifer suggested by Guglielmi et al. (2002).

6. Concluding remarks

For the first time, a geophysical study has been carried out at the summit of the La Clapière landslide. It illustrates clearly that electrical resistivity tomography is very helpful in studying landslides because it not only gives a resistivity value which depends upon the physical and hydrological parameters of the materials, but it also provides information upon specific geoelectrical heterogeneity of the investigated zone and, thus, upon its lithological variations. At the first site (on the East flank of the slope), the geophysical data (resisitivity and velocity of the P-wave) allowed a characterisation of the quality of the rock and to distinguish between weathered and unweathered materials. A weathered material is characterised by a true resistivity value lower than 2000±500 Ω m and/or P-wave velocity lower than 2000 m/s. This characterisation was then used to interpret 2D images obtained by the electrical resistivity tomography technique. These images have shown that the superficial part of the slope is likely to be strongly fractured over a thickness ranging from a few meters to 30 m. They showed also the importance of the weathering and the complexity of groundwater movement within the slope. Indeed, the very low resistivities of the materials (<300±100 Ω m) compared to those from weathered rock (2000±500 Ω m) can be interpreted as a saturated layer. Thus, the origin of the instability of the upper part of the La Clapière landslide may be associated with groundwater circulation. The maximum depth of the slipping surface at the landslide can also be derived from the electrical tomography profiles and was found to be around 30 m.

Moreover, we have for the first time investigated the vertical structure of the La Clapière landslide at depth. From the pole–pole survey, we detected a very strong decreasing of the resistivity to a depth of approximately 90 m. The material below this limit is characterised by very low resistivity of about 100 Ω m which suggests the presence of a perched aquifer. This boundary could be associated to the main shear surface of the La Clapière landslide for this altitude. This information is very important because this saturated material could be responsible for the destabilization of the massif. It is clear that 3D surveying with multi-electrode arrays would be a useful addition to this study in order to obtain a complete spatial structure. In the future these data will be used for a stability assessment of the area.

Acknowledgements

We acknowledge O. Kuras and an anonymous reviewer for comments and suggestions to improve this contribution. The authors also thank Veronique Pisot for drafting the figures and Christopher Wibberley for his English review and comments. This study has been supported by PNRN 2002, ACI CatNat 2003, and ACI SAMOA 2004.

References

Bear, L.P., Hohmann, G.W., Tripp, A.C., 1996. Fast resistivity/IP inversion using a low-contrast approximation. Geophysics 61, 169–179.

Cappa, F., Guglielmi, Y., Soukatchoff, V.M., Mudry, J., Bertrand, C., Charmoille, A., 2004. Hydromechanical modelling of a large moving rock slope inferred from slope levelling coupled to spring long-term hydrochemical monitoring: example of the La Clapière landslide (Southern Alps, France). Journal of Hydrology 291, 67–90.

Casson, B., Delacourt, C., Baratoux, D., Allemand, P., 2003. Seventeen years of the "La Clapière" landslide evolution analysed from ortho-rectified aerial photographs. Engineering Geology 68 (1–2), 123–139.

Catani, F., Farina, P., Moretti, S., Nico, G., Strozzi, T., 2005. On the application of SAR interferometry to geomorphological studies: estimation of landform attributes and mass movements. Geomorphology 66, 119–131.

Chigira, M., Wang, W.-N., Furuya, T., Kamai, T., 2003. Geological causes and geomorphological precursors of the Tsaoling landslide triggered by the 1999 Chi-Chi Earthquake, Taiwan. Engineering Geology 68, 259–273.

Compagnon, F., Guglielmi, Y., Mudry, J., Follacci, J.P., Ivaldi, J.P., 1997. Approche chimique et isotopique de l'origine des eaux en transit dans un grand glissement de terrain: Exemple du glissement de la Clapière (Alpes-Maritimes). Comptes Rendus de l'AcadeÂmie des Sciences, Paris 565–570 (325 II).

Costet, J., Sanglerat, D., 1981. Cours pratique de mécanique des roches. Edt Dunod, Paris.

D'amato Avanzi, G., Giannecchini, R., Puccinelli, A., 2004. The influence of the geological and geomorphological settings on shallow landslides. An example in a temperate climate environment: the June 19, 1996 event in northwestern Tuscany (Italy). Engineering Geology 73, 215–228.

Delteil, J., Stephan, J.-F., Attal, M., 2003. Control of Permian and Triassic faults on Alpine basement deformation in the Argentera massif

(external southern French Alps). Bulletin de la Société géologique de France 174, 55–70.

Dymond, J.R., Ausseil, A.-G., Shepherd, J.D., Buettner, L., 2006. Validation of a region-wide model of landslide susceptibility in the Manawatu-Wanganui region of New Zealand. Geomorphology 74, 70–79.

Edwards, L.S., 1977. A modified pseudosection for resistivity and induced-polarization. Geophysic 42, 1020–1036.

Follacci, J.P., 1987. Les mouvements de versant de La Clapière à Saint-Etienne de Tinée (Alpes Maritimes). Bulletin de Liaison des Laboratoires des Ponts et ChausseÂes 150/151, 107–109.

Follacci, J.P., 1999. Seize ans de surveillance du glissement de La Clapière (Alpes Maritimes). Bulletin de Liaison des Laboratoires des Ponts et Chausseés 220, 35–55.

Godio, A., Bottino, G., 2001. Electrical and electromagnetic investigation for landslide characterisations. Physics and Chemistry of the Earth 26, 705–710.

Godio, A., Strobbia, C., De Bacco, G., 2006. Geophysical characterisation of a rockslide in an alpine region. Engineering Geology 83, 273–286.

Guglielmi, Y., Mudry, J., Blavoux, J., 1998. Estimation of the water balance of alluvial aquifers in a high isotopic contrast region: an example from Southeastern France. Journal of Hydrology 210, 106–115.

Guglielmi, Y., Bertrand, C., Compagnon, F., Follacci, J.P., Mudry, J., 2000. Acquisition of water chemistry in a mobile fissured basement massif: its role in the hydrogeological knowledge of the La Clapiere landslide (Mercantour massif, southern Alps, France). Journal of Hydrology 229, 138–148.

Guglielmi, Y., Vengeon, J.M., Bertrand, C., Mudry, J., Follacci, J.P., Giraud, A., 2002. Hydrogeochemistry: an investigation tool to evaluate infitration into large moving rock masses (Case study of the La Clapière and Séchilienne alpine landslides). Bulletin of Engineering Geology and the Environment 61, 311–324.

Guglielmi, Y., Cappa, F., Binet, S., 2005. Coupling between hydrogeology and deformation of mountainous rock slopes: insight from La Clapière area (Southern-Alps, France). Comptes Rendus, Géosciences 337, 1154–1163.

Gunzburger, Y., Laumonier, B., 2002. Origine tectonique du pli supportant le glissement de terrain de la Clapière (Nord-Ouest du massif de l'Argentera-Mercantour, Alpes du Sud, France) d'après l'analyse de la fracturation. Comptes Rendus Geosciences 334, 415–422.

Hutchinson, J.N., 1988. General report: morphological and geotechnical parameters of landslides in relation to geology and hydrology. In: Bonnard, C. (Ed.), Proc., 5th International Symposium on Landslides, vol. 1A. Balkelma, Rotterdam, Netherlands, pp. 3–35.

Ivaldi, J.-P., Guardia, P., Follacci, J.-P., Terramorsi, S., 1991. Plis de couverture en échelon et failles de second ordre associés à un décrochement dextre de socle sur le bord nord-ouest de l'Argentera (Alpes-Maritimes, France). Comptes Rendus de l'AcadeÂmie des Sciences Paris, Série II 313, 361–368.

Jongmans, D., Hemroulle, P., Demanet, D., Renardy, F., Vanbradant, Y., 2000. Application of 2D electrical and seismic tomography techniques for investigating landslides. European Journal of Environmental & Engineering Geophysics 5, 75–89.

Komac, M., 2006. A landslide susceptibility model using the analytical hierarchy process method and multivariate statistic in perialpine Slovenia. Geomorphology 74, 17–28.

Lebourg, T., Frappa, M., 2001. Mesures géophysiques pour l'analyse des glissements de terrain. Revue Française de Géotechnique 95/96, 33–40.

Lebourg, T., Frappa, M., Sirieix, C., 1999. Reconnaissance des surfaces de rupture dans les formations superficielles instables par mesures électriques. PANGEA 31, 69–72.

Lebourg, T., Tric, E., Guglielmi, Y., Cappa, F., Charmoille, A., Bouissou, S., 2003. Geophysical survey to understand failure mechanisms involved on Deep Seated Landslides. EGS, Nice.

Lebourg, T., Riss, J., Pirard, E., 2004. Influence of morphological characteristics of heterogeneous moraine formations on their mechanical bahaviour using image and statistical analysis. Engineering Geology 73, 37–50.

Lebourg, T., Binet, S., Tric, E., Jomard, J., El Bedoui, S., 2005. Geophysical survey to estimate the 3D sliding surface and the 4D evolution of the water pressure on part of a Deep Seated Landslide. Terra Nova 17, 399–406.

Loke M.H., 1997. Res2DINV software user's manual.

Loke, M.H., Barker, R.D., 1996. Rapid least-squares inversion of apparent resistivity 455 pseudosections by a quasi-Newton method. Geophysical Prospecting 44, 131–152.

Mauritsch, H.J., Seibert, W., Amdt, R., Römer, A., Schneiderbauer, K., Sendlhofer, G.P., 2000. Geophysical investigations of large landslides in the Carnic region of Southern Austria. Engineering Geology 56, 373–388.

Merrien-Soukatchoff, V., Quenot, X., Guglielmi, Y., 2001. Modélisation par éléments distincts du phénomène de fauchage gravitaire. Application au glissement de la Clapière (Saint-Etienne-de-Tinée, Alpes-Maritimes). Revue Française de Géotechnique 95/96, 133–142 ISBN 0181-0529.

Perrone, A., Iannuzzi, V., Lapenna, P., Lorenzo, S., Piscitelli, E., Rizzo, Sda, F., 2004. High-resolution electrical imaging of the Varco d'Izzo earthflow (southern Italy). Journal of Applied Geophysics 56, 17–29.

Rey, E., Jongmans, D., Gotteland, P., Garambois, S., 2006. Characterisation of soils with stony inclusions using geoelectrical measurements. Journal of Applied Geophysics 58, 188–201.

Ritz, M., Parisot, J.-C., Diouf, S., Beauvais, A., Dione, F., Niang, M., 1999. Electrical imaging of lateritic weathering mantles over granitic and metamorphic basement of eastern Seneag, West Africa. Journal of Applied Geophysics 41, 335–344.

Robain, H., Descloitres, M., Ritz, M., Atangana, Q.Y., 1996. A multiscale electrical survey of a lateritic soil in the rain forest of Cameroon. Journal of Applied Geophysics 34, 237–253.

Roth, M.J.S., Mackey, J.R., Mackey, C., Nyquist, J.E., 2002. A case study of the reliability of multielectrode earth resistivity testing for geotechnical investigations in karst terrains. Engineering Geology 65, 225–232.

Squarzoni, C., Delacourt, C., Allemand, P., 2003. Nine years of spatial and temporal evolution of the La Valette landslide observed by SAR interferometry. Engineering Geology 68 (1–2), 53–66.

Sumanovac, F., 2006. Mapping of thin sandy aquifers by using high resolution reflection seismic and 2-D electrical tomography. Journal of Applied Geophysics 58, 144–157.

Sumanovac, F., Weisser, M., 2001. Evaluation of resistivity and seismic methods for 480 hydrogeological mapping in karst terrains. Journal of Applied Geophysics 47, 13–28.

Wise, D.J., Cassidy, J., Locke, C.A., 2003. Geophysical imaging of the quaternary Wairoa north fault, New Zealand: a case study. Journal of Applied Geophysics 53, 1–16.